Effect of Protonation and PAMAM Dendrimer Size on the Complexation and Dynamic Mobility of 2-Naphthol

Mark H. Kleinman,[†] James H. Flory,[†] Donald A. Tomalia,[‡] and Nicholas J. Turro*,[†]

Department of Chemistry, Columbia University, 3000 Broadway, Mail Code 3119, New York, New York 10027, and Center for Biologic Nanotechnology, University of Michigan, 4027 Kresge II, 200 Zina Pitcher Place, Ann Arbor, Michigan 48109-0533

Received: May 22, 2000; In Final Form: August 24, 2000

The supramolecular dynamics of triplet excited states of the 2-naphthol@dendrimer (2-NpOH@*n*-SBD) noncovalently bound complex have been studied by fluorescence spectroscopy and laser flash photolysis. By varying the acidity and dendrimer size, polyamidoamine dendrimers are shown to possess both nonspecific and specific binding properties. For example, the studies show that 2-naphthol binds preferentially to the tertiary amine groups within the dendrimer interior and can be released by lowering the pH of the solution. On a per binding site basis, studies of the dynamics of ^{3}2-NpOH*@*n*-SBD reveal that the overall dynamics (entry and exit rate constants) are enhanced by increasing the acidity of the solution. Furthermore, the amount of protonation of tertiary amine groups within 2-SBD, 4-SBD, and 6-SBD was determined to be ~12%, ~10%, and <1%, respectively, at pH 6. The results presented here demonstrate that, in addition to being able to complex transition metals, organic molecules that are capable of hydrogen bonding to the internal amine moieties can also be bound to dendrimers.

Introduction

Complexation Dynamics in Supramolecular Dendritic Systems. Polyamidoamine (PAMAM) dendrimers[1] are polymers composed of a central core (ethylenediamine in this study) with amidoamine branching units that extend outward in a symmetric fashion and consist of generations (*n*, layers) of these units. As such, the dendrimers contain both primary amines located in the outermost shell as well as amides and tertiary amines throughout the interior (Figure 1). The structural characteristics of these dendrimers have been well studied. In particular, it is worth noting that, as the generation of dendrimer increases, a substantial change in structure is typically observed around 4-SBD.[1] Below 4-SBD, dendrimers are open and elongated, whereas above 4-SBD, they tend to be spherical and have densely packed outer shells.[1] PAMAM dendrimers have been proposed for use in many areas of medical and health science (drug delivery,[2] MRI contrast agents,[3] and gene transfection).[4,5] In addition, dendrimers have also served as models for histones,[6] surfactants,[7−9] catalysts,[10] environmental cleanup agents,[11] and nanomaterials.[12,13] Of particular interest to this report are the recent publications that have highlighted the use of dendrimers as delivery systems for small hydrophobic molecules that are released as the pH is lowered.[2,14,15]

Previous studies have compared larger dendrimers with micelles because both systems can act as supramolecular host molecules capable of binding small guest molecules (guest@host complexes).[9] Photochemical and photophysical probing techniques have been widely used to explore the structural properties of the host systems.[16−18] In the case of drug delivery or environmental cleanup agents, direct rate constants are required to evaluate not only the "tightness" of binding (*K*) but also the rate of movement between the complexation agent and the surrounding fluid environment.

PAMAM dendrimers have an outer shell of primary amines with a pK_a in the range of 7−9 and internal, tertiary amine moieties with pK_a values between 3 and 6.[19] Since the pH of the solution can be varied, the number of unprotonated amines available for complexation by a proton donor can also be manipulated. Here, we use 2-naphthol (2-NpOH) as a probe that is capable of recognizing the dendrimer amines by forming hydrogen bonds.[20]

Photophysics of ^{1}2-NpOH*. The ground-state acidity constant (pK_a) of 2-NpOH is 9.3, whereas the pK_a of the excited state (^{1}2-NpOH*) is 2.9 (Scheme 1).[21] Previous studies of the photophysics of ^{1}2-NpOH* have shown that the neutral form deprotonates, yielding the anionic naphthoate, which emits at λ_{max} = 430 nm, while the neutral form fluoresces with λ_{max} = 360 nm. The pH of the local environment around 2-NpOH determines the relative emission quantum yields.[22]

Using Excited States to Investigate Dynamic Processes. Evaluation of dynamic processes can be furnished by using excited states, provided that the rate of the diffusive process being monitored is on the same order of magnitude as the rate of decay of the excited state.[23] In the case of ^{1}2-NpOH*, the neutral naphthol and anionic naphthoate species have emission lifetimes of less than 10 ns in water.[24] Since the rate of decay of these fluorescent species is fast relative to diffusion in and out of supramolecular systems, the dynamic rate constants for the reporter molecule cannot be made by directly studying the fluorescence. In contrast, the lifetimes of triplet excited states are much longer (microseconds). On this time scale, the probe molecule is expected to have enough time to diffuse in and out, as well as within, the macromolecular system.

Only a few studies that explore the properties of triplet excited 2-naphthol (^{3}2-NpOH*) have been carried out.[20,25] The differ-

* To whom correspondence should be addressed: Fax (212) 932-1289. E-mail: turro@chem.columbia.edu.
[†] Columbia University.
[‡] University of Michigan.

10.1021/jp001882r CCC: $19.00
Published on Web 00/00/0000 PAGE EST: 7.8

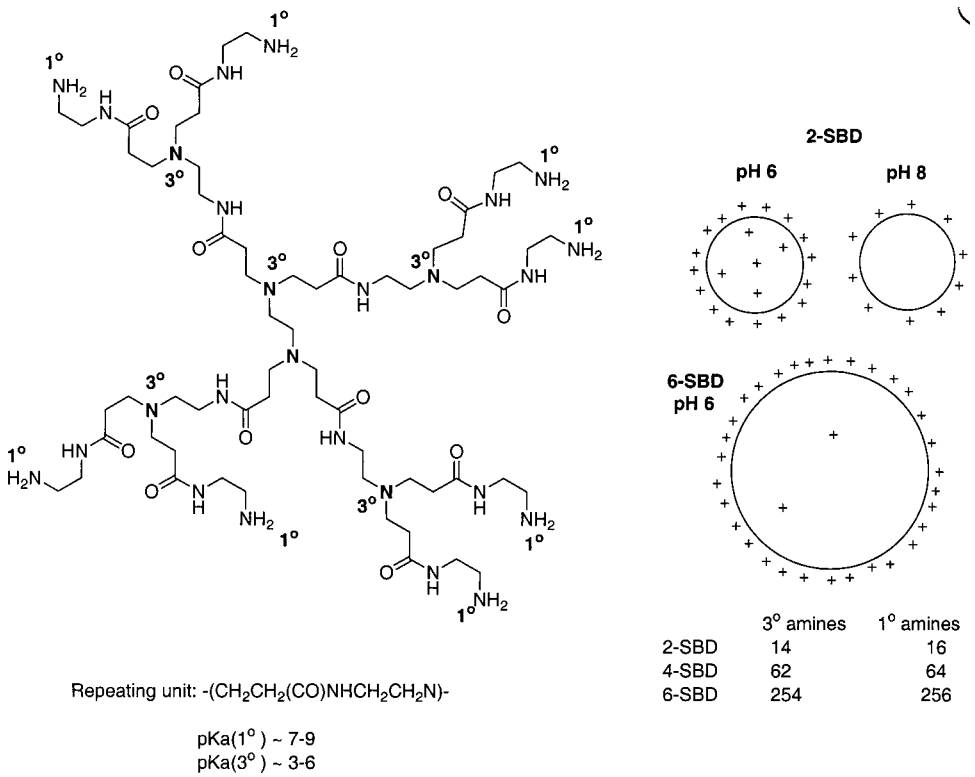

Figure 1. Composition and structural features of ethylenediamine core PAMAM dendrimers. The structure of a 1-SBD PAMAM dendrimer with an ethylenediamine core is shown at left. A conceptual illustration of the levels of protonation in 2-SBD and 6-SBD at pH 6 and 8 is shown at right. In addition, the number of amines in each generation used in this study and approximate pK_a ranges are shown. Acidity constants were taken from ref 1.

SCHEME 1: Kinetic Scheme Depicting the Proton Transfer Properties of 2-NpOH upon Excitation[a]

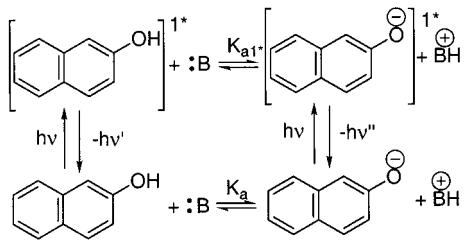

[a] Note that the excited state K_{a1*} is much larger than the ground state K_a.

ence in acidity between the ground state (pK_a = 9.3) and the excited triplet state (pK_a = 8.1) is much smaller than the difference between the pK_a the ground state and the excited singlet state (pK_a = 2.9). In this study, we use features of molecular recognition[26] to noncovalently bind 2-naphthol (2-NpOH) to small (2-SBD), medium (4-SBD), and large (6-SBD) dendrimers. Fluorescence spectroscopy is used to determine the binding site of the 2-naphthol@dendrimer interaction. In conjunction with these studies, we utilize the triplet excited state of 2-naphthol (^{3}2-NpOH*) to monitor the complexation dynamics and to evaluate the rate of exit (k_-) and entry (k_+) into the dendrimer host system as a function of pH.

Materials and Methods

2-Naphthol (Acros, 99+%) was recrystallized from ethanol and water. Deionized water was obtained using a Millipore filtration system. Triethylamine (Fisher, peptide synthesis grade), ethylenediamine (Aldrich, 99.5%), triethanolamine (Aldrich, 98%), and *N*-methylacetamide (Aldrich, 99+%) were used as received. Sodium nitrite (Aldrich, 99.99%), sodium hydrogen phosphate heptahydrate (99.99+%), sodium dihydrogen phosphate monohydrate (Aldrich 98%), and standard pH buffers (Fisher) were used without additional purification.

The synthesis of PAMAM dendrimers has been reported elsewhere.[19] PAMAM dendrimers were obtained in methanolic stock solutions from Dendritech (Midland, MI). Solutions of PAMAM dendrimers were generated by taking a portion of the methanolic stock solution, drying the dendrimers to a film with a stream of argon, and then placing the dendrimers in a vacuum oven (~0.01 Torr) at room temperature overnight. The dendrimers were then diluted with an appropriate volume of pH-adjusted 0.1 M phosphate buffer in deionized water to reach the desired concentration. To produce a solution containing 2-NpOH@dendrimer, an aliquot of a filtered (Millex-PF, 0.8 μm), saturated solution of 2-NpOH in water was added into the dendrimer solution. The final absorbance at 308 nm was in the range of 0.3−0.5 (~50 μM). The solutions were then allowed to equilibrate overnight with magnetic stirring.

pH values were obtained on a Corning pH meter 220 standardized at pH 4 and 7. UV−vis spectra were measured on a HP 8452A diode array spectrometer using quartz cells with path lengths of 1.0 cm. Emission spectra were recorded either on a Spex Fluorolog 1680 0.22 m double spectrometer or a Spex FluoroMax-2 spectrometer using quartz cells with path lengths of 1.0 cm. For the emission spectra, a wavelength interval of 1 nm and integration time of 1 s were used. Emission intensities taken for quenching plots were taken with an integration time of 2 s.

Laser flash photolysis experiments employed pulses (XeCl, 308 nm, <30 mJ/pulse, pulse duration of 5−10 ns) from a Lambda Physik 50 excimer laser. The system and data acquisition process have been described elsewhere.[27] Unless otherwise stated, in all transient absorption experiments the solutions were

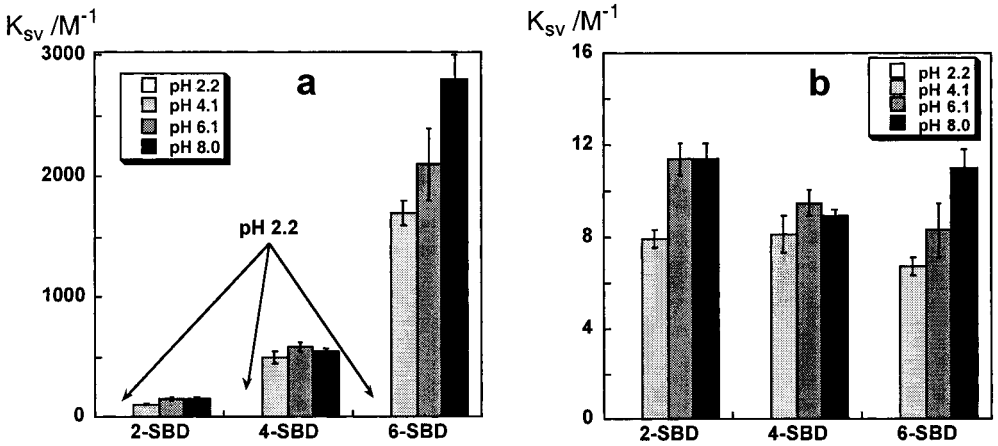

Figure 2. Stern−Volmer constants in units of M^{-1} derived from fluorescence quenching studies of ^{1}2-NpOH* at different pH values in PAMAM dendrimers of varying generations (2-SBD, 4-SBD, and 6-SBD). (A) K_{sv} on a per dendrimer basis; (B) K_{sv} per tertiary amine. See the text for more details. The errors represent average deviations from two trials.

deoxygenated by bubbling argon through the solution for at least 30 min. For the quenching experiments where the rate of decay is measured at a single wavelength, 3.0 mL of the 2-NpOH/dendrimer solution was placed in a 1 cm × 1 cm Suprasil quartz cell. Fresh samples were prepared for each experiment. The deoxygenated quencher solution was added to the initial solution and shaken to ensure complete mixing. At each quencher concentration, six laser shots were obtained and the results were averaged. No photodecomposition over the course of each quenching experiment was evident for 2-NpOH in water or PAMAM dendrimers at pH >4 as judged from the lack of change in the ground-state UV−vis spectrum before and after photolysis. For transient absorption spectra, a total volume of 25 mL was used in a static 1 cm × 1 cm Suprasil quartz cell with additional holding capacity and the sample was shaken between every wavelength that was monitored. No difference in the ground-state UV−vis spectrum before and after photolysis was observed.

Results

Fluorescence Spectroscopy. In the case of 2-NpOH emission experiments, a quenching methodology is used whereby an extrinsic deactivator of the excited state is added to the 2-NpOH or 2-NpOH@dendrimer system. For steady-state fluorescence studies, the Stern−Volmer relationship ($I_o/I = 1 + K_{sv}[Q]$) can be applied where [Q] is the concentration of quencher, and I_o and I are the fluorescence intensities in the absence and presence of quencher, respectively. K_{sv} is the Stern−Volmer constant and is equal to $k_{qs}\tau$, where k_{qs} is the quenching rate constant and τ is the intrinsic lifetime of ^{1}2-NpOH* fluorescence. In the absence of dendrimer, I_o/I monitored at 350 nm (emission from the neutral species) increases linearly with increasing [Q]. Addition of PAMAM dendrimers to a 2-NpOH solution resulted in a linear decrease in fluorescence intensities. All quenching plots had 8−15 points and had r^2 values greater than 0.97. The experiments were carried out with maximum dendrimer concentrations of 0.06, 0.25, and 1 mM for 6-SBD, 4-SBD, and 2-SBD, respectively. These concentrations correspond to 0.03 M in total dendrimer amines. The Stern−Volmer constants derived from the change of the fluorescence intensities at 350 nm (neutral 2-NpOH) are shown in Figure 2. In these experiments, the pH was held constant to within 0.05 pH units.

Figure 2a shows that, on a per dendrimer basis, the Stern−Volmer constant increases with generation. However, when normalized for the number of tertiary amines (Figure 2b), no significant change in the quenching efficiency is observed. Note that the singlet lifetime of the neutral ^{1}2-NpOH* remains relatively constant over the range of pH values studied here,[24] so the changes reflect shifts in k_{qs}. These results indicate that a specific moiety of the dendrimer whose number is proportional to the generation is acting as the quencher of 2-NpOH fluorescence.

Since the primary and tertiary dendrimer amines have different pK_a values, pH-dependent quenching provides insight into the identity of the excited-state deactivator. At pH 2.2, no quenching of the ^{1}2-NpOH* was observed for any generation. This indicates that no interaction between 2-NpOH and the portion of the dendrimer that can deactivate ^{1}2-NpOH* is occurring under the conditions employed. For the smaller generations (2-SBD and 4-SBD) above pH 4, little quenching with no significant pH dependence is seen. In an effort to determine which functional groups of the dendrimer induce the quenching of ^{1}2-NpOH* fluorescence, quenching studies of ^{1}2-NpOH* by triethylamine (pK_a = 10.7), ethylenediamine (pK_{a1} = 6.8 and pK_{a2} = 9.9), triethanolamine (pK_a = 7.8), and *N*-methylacetamide were carried out. Experiments conducted where the pH > p$K_{a(2-NpOH)}$ ~ 9.5 cannot be directly compared to the quenching studies involving the neutral species, because the emitting species is predominantly 2-naphthoate; thus, only experiments where pH <9 were attempted. Results from quenching experiments below the pK_a of triethylamine, triethanolamine, and ethylenediamine show that no significant quenching occurs when the amine group(s) are protonated. The Stern−Volmer constant for *N*-methylacetamide was less than 2 M^{-1}, indicating that minimal quenching by the amide moieties is occurring. As the pH increases, the efficiency of quenching of ^{1}2-NpOH* by the model primary and tertiary amines also increases. Furthermore, the amines have a Stern−Volmer constant approximately equal to that of the dendrimers on a per amine basis. These results suggest that 2-NpOH binds to the dendrimer amines that have a pK_a in the range of 3−6. This is in the same pH range where the tertiary amines are expected to become protonated. In contrast, the primary amines generally protonate within a pH range of 6−9.[19,28]

Transient Absorption Spectroscopy. Some of the characterization of ^{3}2-NpOH* has been covered in work by others,[20,25,29] so here we concentrate on the properties of ^{3}2-NpOH* as required to understand the nature of experiments conducted in dendritic systems.

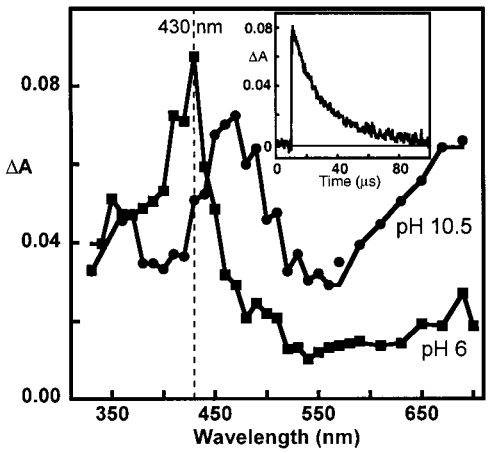

Figure 3. Transient absorption spectra of 2-NpOH in water at pH 6 and 10.5. The spectra were taken 1.3 and 1.1 μs after the laser pulse, respectively. The broad spectral band >650 nm is attributed to the hydrated electron, the peak at 430 nm to ^{3}2-NpOH*, and the other bands to the naphthoxyl radical or a combination of ^{3}2-NpOH* and naphthoxyl radical. A representative decay for 2-naphthol in water at pH 6 monitored at 430 nm is shown in the inset.

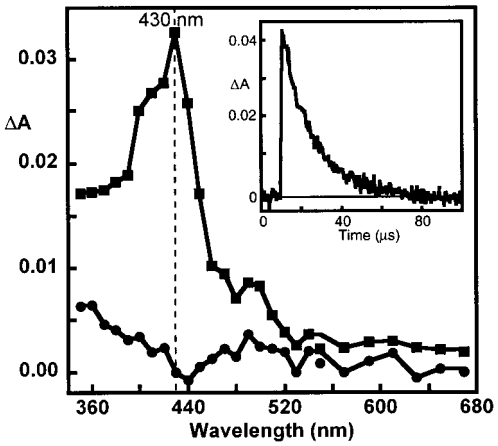

Figure 4. Transient absorption spectrum of ^{3}2-NpOH*@6-SBD at pH 6 The spectra were taken 12.5 μs (■) and 50 μs (●) after the 308 nm laser pulse, respectively. The inset shows a representative decay for ^{3}2-NpOH*@6-SBD at pH 6 monitored at 430 nm. Transient absorption spectra obtained in the case of ^{3}2-NpOH*@2-SBD and ^{3}2-NpOH*@4-SBD were similar to those shown above.

Figure 3 shows the transient absorption spectrum taken 1.3 μs after a 308 nm laser pulse with a deoxygenated solution of 2-NpOH in water at pH 6 and 10.5.

Oxygen is a known deactivator of triplet excited states. By saturating the solution with oxygen, the spectral signal at 430 nm is eliminated, but the signals at 480 and 350 nm persist. On the basis of experiments by others[25,29] and the oxygen quenching experiments, the peak at 430 nm is attributed to ^{3}2-NpOH* and the neighboring bands to 2-NpO• or a combination of ^{3}2-NpOH* and 2-NpO•. No growth kinetics for the formation of 2-NpO• are observed, because the biphotonic process of ionization that leads to radical formation probably occurs during the laser pulse. Bubbling of N_2O, an efficient hydrated electron scavenger, into the sample eliminates the band at >650 nm, while leaving the other bands intact. The efficient quenching of the broad signal at >650 nm by N_2O allows us to ascribe this band to the hydrated electron. In argon-saturated solutions, at pH 6, the lifetimes of 2-NpO•, ^{3}2-NpOH*, and the hydrated electron are 48, 25, and 1 μs, respectively. The lifetime of ^{3}2-NpOH* at pH 6 and at pH 8 was identical within experimental error and increased to 40 μs at even lower pH values. Since the pK_a of ^{3}2-NpOH* is 8.1, the processes monitored at lower pH values are ascribed to neutral ^{3}2-NpOH*. At the same energy per pulse, the quantum yield of electron ejection from 2-NpO− is dramatically increased compared with that of 2-NpOH. This may cause the increased rate of photodecomposition observed in aqueous solutions where pH > p$K_{a(2-NpOH)}$.

In buffered solution, the lifetime of ^{3}2-NpOH*@*n*-SBD is 20 μs and does not change significantly with pH or dendrimer generation. Figure 4 shows the time-dependent transient absorption spectra of ^{3}2-NpOH*@6-SBD. No differences were seen for the smaller generations studied. Figure 4 shows that the lifetime of the spectral band at 430 nm (^{3}2-NpOH*) decays with a shorter lifetime than 2-NpO• (480 nm).

For the time-resolved transient absorption studies, where rate constants are determined, a modified Stern−Volmer equation in the form of $k_{obs} = k_o + k_q[Q]$ is used to determine the quenching rate constant, k_q, where k_{obs} is the observed rate constant of decay of ^{3}2-NpOH*, and k_o is the intrinsic rate of decay of ^{3}2-NpOH* in the absence of quencher. In homogeneous solution such as water, a plot of the dependence of k_{obs} on quencher concentration yields a straight line with a slope of k_q. Experiments where either protonated ethylenediamine or protonated triethylamine (pH < pK_a) were added to aqueous solutions of 2-NpOH resulted in $k_q \leq 10^6$ M^{-1} s^{-1}. Furthermore, experiments whereby concentrated dendrimers solutions (n = 2, 4, 6-SBD) were added into a 2-NpOH solution also yielded $k_q \leq 10^6$ M^{-1} s^{-1}. These observations agree with other work,[20] where protonated amines were found to be poor quenchers of ^{3}2-NpOH*.

In the case of microheterogeneous systems where a guest@host complex exists, the quencher may not have access to all regions of the host macromolecule. For example, in the case of a small, highly water soluble cationic quencher and cationic micelle, the quencher will tend to reside in the aqueous phase due to the electrostatic repulsion from the micelle surface. Studies on the dynamics of triplet excited states and quenchers have been employed to investigate both surfactant self-assemblies and direct host−guest complexes such as cyclodextrins.[30−36] The model (eq 1) requires that different quenching efficiencies exist for the probe in water and for the probe within the macromolecular host (H). Key assumptions in this model are that (1) the concentration of free probe is small compared to the concentration of complexed probe (*P*), (2) the excited triplet state does not decay in the water phase by any process other than deactivation by the quencher, (3) the decay of the probe must follow pseudo-first-order kinetics for all quencher concentrations, and (4) the guest@host complex has a 1:1 stoichiometry. Under these conditions, eq 1 has been derived[36]

$$k_{obs} = k_h + k_{p-} + k_{qh}[Q] - \frac{k_{p-} + k_{p+}[H]}{k_{p+}[H] + k_o + k_{qo}[Q]} \quad (1)$$

where k_h and k_o are the decay rate constants for ^{3}2-NpOH*@*n*-SBD and free ^{3}2-NpOH*, respectively. k_{p-} and k_{p+} are the exit and entry rate constants of ^{3}2-NpOH*@*n*-SBD. k_{qo} and k_{qh} are the quenching rate constants in water and inside the supramolecule, respectively. If large enough quencher concentrations are used, the last term in eq 1 is rendered negligible and the k_{obs} becomes equal to $k_h + k_{p-} + k_{qh}[Q]$. In addition to quantitative analysis, by its shape, a quenching plot can qualitatively illustrate the relative amount of access of a quencher to the guest. For example, different curvatures are evident for quenching processes where the quencher has little or no access to the probe within the host [$k_{qh}[Q] \ll (k_h + k_{p-})$]

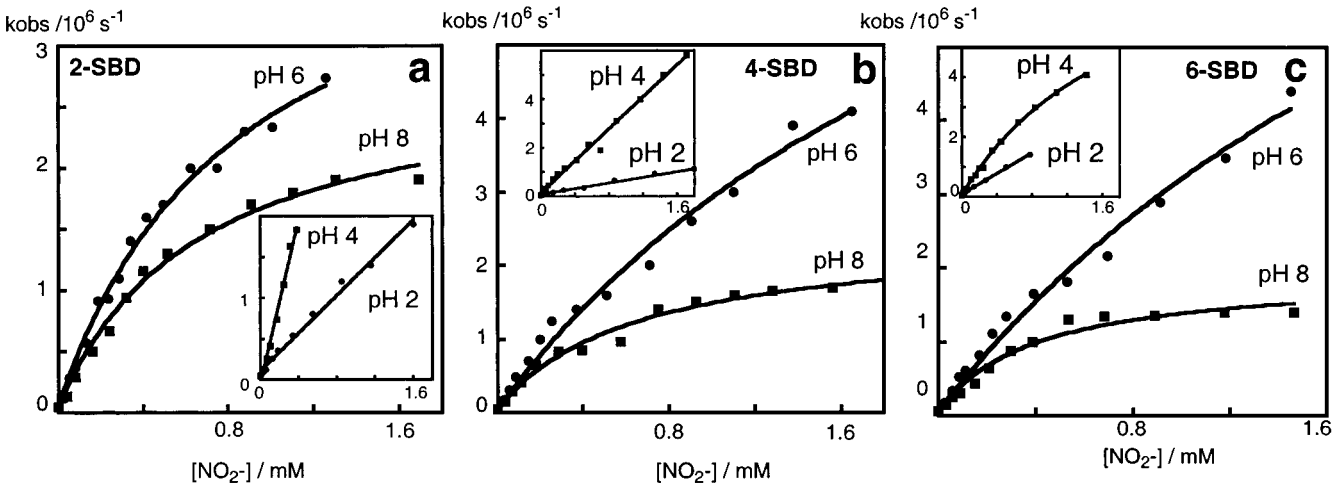

Figure 5. Quenching of (a) ^{3}2-NpOH*@2-SBD (1 mM), (b) ^{3}2-NpOH*@4-SBD (0.28 mM), and (c) ^{3}2-NpOH*@6-SBD (0.07 mM) by NO_2^- in solutions of pH 6 (●) and pH 8 (■). The number of dendrimer amines is kept constant in all experiments above. The best fit curves were generated as described in the text. The insets display the quenching of ^{3}2-NpOH* by NO_2^- at pH 2 (●) and pH 4 (■) for each generation. The axes for the insets are k_{obs} (s^{-1}) and [NO_2^-] (mM).

and where the efficiency of quenching within the host (k_{qh}[Q]) is significant.

In an effort to minimize quenching inside the dendrimer, one can employ a quencher with the same charge as the surface. However, amines are known to complex many transition metals, and in fact, recent work has shown that PAMAM dendrimers have a high affinity for metals such as copper and cobalt.[11,37−39] For this reason, this approach could not be fully utilized, and nitrite,[30] a highly water soluble, anionic quencher, was chosen. The main limitation in the use of an anionic quencher is that the quencher is attracted to the positively charged surface of the dendrimer and may deactivate the excited-state probe before complete exit from the macromolecule.

In buffered water solutions with pH values between 4 and 8, the quenching rate constant of ^{3}2-NpOH* by nitrite was found to be pH independent and equal to $(3 \pm 1) \times 10^9$ M^{-1} s^{-1} (Supporting Information). Nitrite decomposes in acidic solutions,[40] so as a control, a fresh solution of the quencher was prepared at pH 2 and used within an hour of being generated. Using this solution, a quenching rate constant of 1×10^9 M^{-1} s^{-1} was obtained, indicating slightly smaller quenching efficiencies. In the absence of dendrimer, at all pH values studied, a strict linear relationship between k_{obs} and [NO_2^-] was observed until no measurable absorptive signal remained.

In the presence of dendrimers, NO_2^- quenching of ^{3}2-NpOH* varied from linearity as shown in Figure 5.

The curvature of the plot increases at higher pH values, which is indicative that NO_2^- has less access to the 2-NpOH@dendrimer complex at higher pH values. Furthermore, curvature is observed at pH 4 for only the largest generation studied (6-SBD). This suggests that the level of protonation inside the dendrimer is still low enough such that 2-NpOH can bind to the interior binding sites. It further suggests that the access of NO_2^- to the 2-NpOH binding site is hindered. In a qualitative manner, the pH dependence of the curvatures in Figure 5 agrees with the fluorescence results (Figure 2), which show that the complexation properties of 2-NpOH change dramatically between pH 3 and 6.

Under conditions in which larger amounts of NO_2^- are added to the 2-naphthol@dendrimer complex, k_{obs} does not change significantly with the addition of even more nitrite. However, the introduction of oxygen into the solution results in a strong reduction of the absorptive signal as well as a large increase in the rate of decay. This indicates that oxygen has access to areas of the dendrimer that nitrite does not and that the dendrimer is capable of protecting the complexed species.

The data were analyzed using eq 1, where the known values for the concentration of *n*-SBD, k_o, and k_{qo} were obtained from different experiments. Independent experiments conducted under conditions where all of the 2-NpOH was assumed to complex to the dendrimer (large excess of dendrimer) were employed to evaluate k_{qh}. At pH 6 and 8, k_{qh} was invariant of dendrimer generation and found to be 3×10^8 and $<10^6$ M^{-1} s^{-1}, respectively. The remaining parameters, k_{p+} and k_{p-}, were the only parameters derived from the curve-fitting procedure. Table 1 lists the rate constants obtained form the curve-fitting process.

On a per dendrimer basis, the data (Table 1) reveal very large, bimolecular k_{p+} values, which depend on the concentration of dendrimer. This concentration takes the number of molecules of dendrimer into consideration, but not the number of amines, which are the actual binding sites for 2-NpOH (vide infra). For example, there are 254 tertiary amines in a single molecule of 6-SBD. The results demonstrate that larger dendrimers can complex a larger number of 2-NpOH molecules. Further, on the basis of the number of teriary amines, an increase in pH increases the number of available binding sites, and thus, a decrease in the entry rate constant is observed. This occurs with a concomitant decrease in the exit rate constant of ^{3}2-NpOH* from the dendrimer macromolecule. At pH 8, where most of the surface amines are expected to be deprotonated, virtually no change in the exit rate constant is observed for all generations for the dendrimer studied. Equilibrium constants for the binding of the ^{3}2-NpOH* to dendrimers can be calculated on the basis of the dynamic rate constants ($K = k_{p+}/k_{p-}$). The equilibrium constants (per dendrimer) get larger as more amines become available for binding due to the dendrimer size and the level of protonation. For instance, for 6-SBD, *K* increases from 7900 to 9400 M^{-1} as the pH of the solution increases from pH 4 to 8. It should also be noted that the values of *K* are relatively large for complexes based on noncovalent interactions.

It has been pointed out that data analyzed as per eq 1 (cf. Figure 5) is limited by the fact that, in many situations, the plateau at higher quencher concentrations is not well-defined and relies heavily on the data taken on the shortest time scales. As such, a double reciprocal plot stemming from eq 2, which is based on a similar model, has been offered as the preferred

TABLE 1: Exit and Entry Rate Constants Determined from the Curve-Fitting Process[a]

	$k_{p+}/10^8$ M^{-1} s^{-1}			$k_{p-}/10^6$ s^{-1}			K (M^{-1})		
dendrimer	pH 4	pH 6	pH 8	pH 4	pH 6	pH 8	pH 4	pH 6	pH 8
2-SBD									
per molecule		19 ± 0.5	16 ± 5		3.6 ± 0.2	2.7 ± 0.2		0.53×10^3	0.59×10^3
per **3**° amine		1.3 ± 0.4	1.1 ± 0.3					36	41
4-SBD									
per molecule		250 ± 70	59 ± 8		11 ± 2	2.4 ± 0.2		2.3×10^3	2.5×10^3
per **3**° amine		4 ± 1	0.95 ± 0.10					36	40
6-SBD									
per molecule	950 ± 100	1000 ± 300	150 ± 30	12 ± 1	12 ± 2	1.9 ± 0.1	7.9×10^3	8.3×10^3	9.4×10^3
per **3**° amine	3.7 ± 0.4	3.9 ± 1.1	0.59 ± 0.12				31	33	33

[a] The concentrations of *n*-SBD were 1×10^{-3}, 2.8×10^{-4}, and 7.0×10^{-5} M for 2-SBD, 4-SBD, and 6-SBD, respectively. k_o, and k_{qo} were set to the 2.7×10^4 s^{-1} and 3×10^9 M^{-1} s^{-1}. For pH 4 and 6, k_{qh} was fixed at the experimentally observed value of 2×10^9 and 3×10^8 M^{-1} s^{-1}, respectively, and assumed to be negligible at pH 8. The results are shown on a per dendrimer molecule and a per 3° amine basis. The magnitude of the rate constants is discussed in the text. Uncertainties in the rate constants were calculated from the average deviation of two experiments and are about 20% for the equilibrium constants.

SCHEME 2: Schematic Overview of the Interaction of 2-NpOH with PAMAM Dendrimers[a]

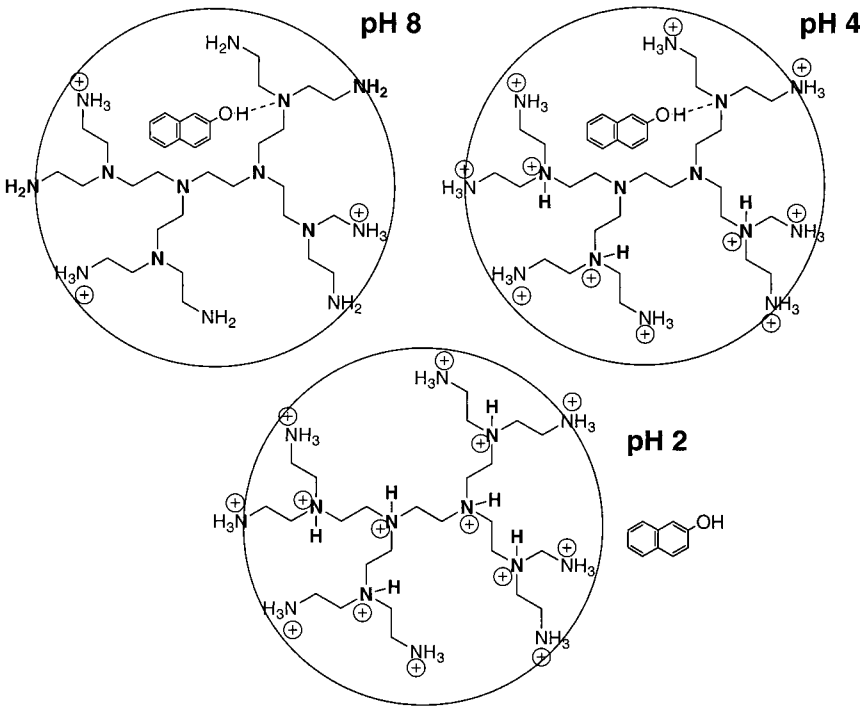

[a] The circle represents the general location of the dendrimer surface. 1-SBD is shown in the illustrated example. As the pH is lowered, the number of binding sites inside the dendrimer is decreased. At pH 2, there are no free 3° amines capable of binding 2-NpOH.

method of analysis.[33,34]

$$\frac{1}{(k_{obs} - k_h)} = \frac{1}{k_-}\left[1 + \frac{k_{p+}[H]}{k_{qo}[Q]}\right] \qquad (2)$$

In this analysis, in addition to the assumptions made in the derivation of eq 1, one assumes that the rate constant for decay of the excited guest molecule (k_o) is small compared to ($k_{p+}[H] + k_q[Q]$). In the 2-NpOH@*n*-SBD system, this has been experimentally verified. Another assumption is that the NO_2^- quencher has no access to the interior of the dendrimer and cannot quench ^{3}2-NpOH* complexed to the dendrimer. The validity of this latter assumption will be analyzed in the Discussion section below. All plots derived from the fitting of the data shown in Figure 5 by eq 2 were strictly linear. The values of k_{p+} and k_{p-} derived from this analysis showed the same trends and typically were within 15% of the value shown in Table 1. This indicates that the binding of NO_2^- to the interior of the dendrimer is minimal.

Discussion

The fundamental approach in this study is to use supramolecular recognition to help understand the complexation dynamics of ^{3}2-NpOH*@*n*-SBD. In aqueous media, a competitive binding process for the amines occurs between protons and 2-NpOH. The key points (Scheme 2) are that 2-NpOH is found to bind to free, unprotonated amines that have a pK_a in the range of 3−6; that on a *per dendrimer* basis the entry rate constant increases with dendrimer size; that the binding constants derived from the analysis of the dynamic behavior increase with increasing pH; and that the exit rate constant decreases with an increase in pH.

In terms of the fluorescence dendrimer quenching experiments, single photon counting fluorescence lifetime measurements reveal that the quenching appears to be static and the process can therefore be ascribed to complexation. The pH dependence of the quenching process in the fluorescence quenching experiments indicate that the dendrimer's 3° functional groups (pK_a = 3−6) can quench the emission of

^{1}2-NpOH* upon binding. Moreover, little change is observed when pH ~ pK_a (1° amines), suggesting that the noncovalently bound 2-NpOH is preferentially bound to the tertiary amines in the dendrimer interior. The complexation of 2-NpOH probably involves the sharing of the 2-NpOH hydroxyl proton by the free amine (Scheme 2). The preference for exclusive complexation to the tertiary amines relative to the primary amines is quite striking but is in line with previous work that showed that the propensity for the formation of hydrogen bonds increases with the number of alkyl substitutions on the amine.[41] In a manner analogous to micelles, in solutions where the tertiary amines remain unprotonated, additional favorable energetics could arise from the hydrophobic effect due to the relatively less polar dendrimer interior compared to that of the polar bulk water.

When studying host@guest systems, it is important to minimize possible interactions between two probe molecules within the same host. As such, the concentration of the 2-NpOH (~50 μM) was kept substantially lower than [*n*-SBD]. As has been done for micelles, a Poisson distribution was used to evaluate the probability of complexation of multiple probes in a single dendrimer.[17] For 2-SBD, greater than 95% of all dendrimers had no 2-NpOH bound, and most of the remaining dendrimers contained a single probe. In the case of the 4-SBD, 85% contained no 2-NpOH, 14% had a single bound probe, and ~1% had two bound probes. The largest dendrimers studies (6-SBD) had 50% of all dendrimers free of 2-NpOH, 35% with one probe and 12% and 3% with two and three probes, respectively. Given the internal volume of 6-SBD, it is unlikely that interactions occur between 2-NpOH probes bound within the same dendrimer.

At this point, it is important to point out that the results from the fluorescence experiments are indicative of ground-state binding, while the laser flash photolysis experiment deals with the 2-NpOH excited triplet state. It has been noted that the dynamics of ground and excited states do differ[32] and that this change might be due to changes in hydrogen-bond basicity.[42] In fact, the increased basicity of ^{3}2-NpOH* could be the initial step leading to exit of the probe from the dendrimer.

In the study of ^{3}2-NpOH* dynamics, the magnitude of the entry rate constants needs to be addressed. Equation 1 is derived on the basis of an implied 1:1 stoichiometry of the guest@host complex. As discussed above, on a per 3° amine basis, the assumption is valid. Both K and k_{p+} (Table 1) depend on the concentration of binding sites. Therefore, it is more reliable to interpret the results in terms of the number of tertiary amines.

In general, one of the limitations of the quenching methodology derived from eq 1 is that the accessibility of the quencher to the ^{3}2-NpOH*@dendrimer must be smaller than the accessibility to ^{3}2-NpOH* in the aqueous phase. On the basis of the double reciprocal analysis at pH 8, minimal quenching of ^{3}2-NpOH* by nitrite within the dendrimer interior was observed. Thus, any binding of nitrite to the dendrimer would have occurred on the external surface. The experiments were carried out with ~18 mM *n*-SBD in surface amines and 1 mM nitrite. Assuming that no nitrite binds to the dendrimer interior and that in acidic solution every NO_2^- complexes to a surface group, then only ~5% of the surface would have a quencher bound to it. Thus, even at the lower pH values employed in the study, complexation of NO_2^- to the dendrimer would play a small role in the quenching of ^{3}2-NpOH*. Furthermore, the fact that O_2 can deactivate ^{3}2-NpOH* with rate constants $>10^9$ M^{-1} s^{-1} even in the presence of relatively large concentrations of NO_2^- (> 1 mM) demonstrates that the excited triplet probe is in an environment that allows fast diffusion of O_2, but not of nitrite. This provides further evidence that NO_2^- is preferentially solubilized in the water rather than in the more hydrophobic interior of the dendrimer. Similar arguments have been raised when iodide was used to quench pyrene in poly(propyleneimine) dendrimers and was found not to penetrate into the interior of the dendrimer.[2] Quantitatively, $k_{qh}(NO_2^-)$ increased as the pH decreased by over 3 orders of magnitude ($<10^6$ to 2×10^9 M^{-1} s^{-1} for pH 8 and 4, respectively). The lack of curvature in the quenching plots at pH 2 (Figure 5) corroborates the results obtained by fluorescence, which show that 2-NpOH does not bind to dendrimers at pH 2 ($K_{SV} \sim 0$ M^{-1}). We can then infer that at pH 2 the NO_2^- quenching of ^{3}2-NpOH* is occurring exclusively in the aqueous phase.

One factor that also needs to be addressed is that of the level of protonation inside the dendritic polymer. A reduced number of 3° amines is available for complexation at pH < pK_a due to their protonation. As shown in Table 1, the k_{p+} values corrected for the change in the number of 3° amines decreased with increasing generation at pH 8 (k_{p+}=1.1×10^8 and 0.59×10^8 M^{-1} s^{-1} for 2-SBD and 6-SBD, respectively). As the size of the dendrimer increases, there are more available binding sites between the core of the polymer and the layer of 1° amines at the surface. As such, it is less probable that 2-NpOH complexes to the binding sites closer to the core. This result is in line with other work, which showed that the area close to the surface of large, neutral dendrimers is quite congested.[1] Furthermore, as the pH increases, on a per binding site basis, the entry rate constants decrease. This change may occur because of the electrostatic repulsion between cationic moieties, which may induce wider gaps between the branches, thereby allowing easier access to the unprotonated amine binding sites. Additional credence to this explanation lies in the increased overall dynamics at pH 6 compared with pH 8 (Table 1).

On a per dendrimer basis, the binding constant for the formation of ^{3}2-NpOH*@*n*-SBD decreases slightly with decreasing pH. Assuming that the interactions involved in the complexation process are similar to those observed in the fluorescence experiments, this result is in line with a competitive binding process between 2-NpOH and protons for the tertiary amines. Using these changes in K, the level of protonation can be estimated. The extent of dendrimer protonation depends highly on the experimental conditions (e.g. temperature and salt concentration) and so is not well established. Other work[19,28] showed that a minimal number of tertiary amines in the dendrimer are protonated at pH 8. On the basis of the assumption that K is based exclusively on 3° unprotonated amines and that at pH 8 no 3° amines are in the protonated form, then an estimate of the number of internal amines that are unprotonated at other pH levels can be obtained. On the basis of the results in Table 1, at pH 6, we estimate that the interior tertiary amines are about 12%, 10%, and <1% protonated for 2-SBD, 4-SBD, and 6-SBD, respectively. Similar behavior has been predicted using simulations and is observed when Mn^{2+} and Cu^{2+} were used to probe the surface and interior of PAMAM dendrimers using EPR spectroscopy.[28,39] In those studies, protonation of smaller sized dendrimers was found to be more probable than for larger dendrimers and the tertiary amines closer to the core were found to have a reduced pK_a relative to identical residues closer to the surface. Therefore, it is reasonable to expect that 2-SBD internal amines are more readily protonated than 6-SBD internal amines.

In summary, we have shown that dendrimers are unique in that they possess properties of micelle systems as well as those

of well-defined receptor systems such as crown ethers. The results provide evidence that 2-NpOH preferentially binds to the tertiary amine groups within the dendrimer interior. Furthermore, as the dendrimer interior becomes increasingly charged, the spacing of the branches may expand, thereby leading to the increased dynamic behavior of the guest molecule. Since larger dendrimers have a greater number of amines that can bind the organic material, the overall binding constant on a per dendrimer basis increases with generation. This study also provides an estimate of the amount of protonation in the dendrimer interior and shows that, at a specific pH, the larger generations of *n*-SBD possess a less charged internal environment than the smaller generations. The results presented here also show that, in addition to being able to complex metal cations, organic material capable of hydrogen bonding to the amine moieties can also be bound.

Acknowledgment. N.J.T. thanks the NSF for support of the research (grant CHE 9812676). This work was supported in part by the National Science Foundation and the Department of Energy under Grant No. NSF CHE 091-367 to the Environmental Molecular Sciences Institute of Columbia University and by the MRSEC Program of the National Science Foundation under Award Number DMR-9809687. M.H.K. thanks the Camille and Henry Dreyfus Foundation and EMSI for a postdoctoral fellowship. J.H.F. is grateful for support from the Rabi Scholar program at Columbia University.

Supporting Information Available: Plots of k_{obs} vs $[NO_2^-]$ in the absence of dendrimers for various pH values. This material is available free of charge via the Internet at http://pubs.acs.org.

References and Notes

(1) Tomalia, D. A.; Naylor, A. M.; Goddard, W. A., III *Angew. Chem., Int. Ed. Engl.* **1990**, *29*, 138−175.
(2) Pistolis, G.; Malliaris, A.; Tsiourvas, D.; Paleos, C. M. *Chem. Eur. J.* **1999**, *5*, 1440−1444.
(3) Tóth, E.; Pubanz, D.; Vauthey, S.; Helm, L.; Merbach, A. E. *Chem. Eur. J.* **1996**, *2*, 1607−1615.
(4) Kukowska-Latallo, J. F.; Bielinska, A. U.; Johnson, J.; Spindler, R.; Tomalia, D. A.; Baker, J. R., Jr. *Proc. Natl. Acad. Sci. U.S.A.* **1996**, *93*, 4897−4902.
(5) Bielinska, A.; Kukowska-Latallo, J. F.; Johnson, J.; Tomalia, D. A.; Baker, J. R., Jr. *Nucl. Acids Res.* **1996**, *24*, 2176−2182.
(6) Chen, W.; Turro, N. J.; Tomalia, D. A. *Langmuir* **2000**, *16*, 15−19.
(7) Turro, N. J.; Barton, J. K.; Tomalia, D. A. *Acc. Chem. Res.* **1991**, *24*, 332−340.
(8) Turro, N. J. *Pure Appl. Chem.* **1995**, *67*, 199−208.
(9) Gopidas, K. R.; Leheny, A. R.; Caminati, G.; Turro, N. J.; Tomalia, D. A. *J. Am. Chem. Soc.* **1991**, *113*, 7335−7342.
(10) Chechik, V.; Crooks, R. M. *J. Am. Chem. Soc.* **2000**, *122*, 1243−1244.
(11) Diallo, M. S.; Balogh, L.; Shafagati, A.; Johnson Jr., J. H.; Goddard, W. A., III; Tomalia, D. A. *Environ. Sci. Technol.* **1999**, *33*, 820−824.
(12) Garcia, M. E.; Baker, L. A.; Crooks, R. M. *Anal. Chem.* **1999**, *71*, 256−258.
(13) Zhao, M.; Tokuhisa, H.; Crooks, R. M. *Angew. Chem., Int. Ed. Engl.* **1997**, *36*, 2596−2598.
(14) Sideratou, Z.; Tsiourvas, D.; Paleos, C. M. *Langmuir* **2000**, *16*, 1766−1769.
(15) Pistolis, G.; Malliaris, A.; Paleos, C. M.; Tsiourvas, D. *Langmuir* **1997**, *13*, 5870−5875.
(16) Balzani, V.; Scandola, F. *Supamolecular Photochemistry*; Ellis Horwood: New York, 1991.
(17) Kalyanasundaram, K. *Photochemistry in Microheterogeneous Systems*; Academic Press: Orlando, FL, 1987.
(18) Ramamurthy, V. *Photochemistry in Organized and Constrained Media*; VCH Publishers: New York, 1991.
(19) Tomalia, D. A.; Baker, H.; Dewald, J.; Hall, M.; Kallos, G.; Martin, S.; Roeck, J.; Ryder, J.; Smith, P. *Polym. J.* **1985**, *17*, 117−132.
(20) Kikuchi, K.; Watarai, H.; Koizumi, M. *Bull. Chem. Soc. Jpn.* **1973**, *46*, 749−754.
(21) Harris, C. M.; Sellinger, B. K. *J. Phys. Chem.* **1980**, *84*, 891−898.
(22) Khuanga, U.; McDonald, R.; Selinger, B. K. *Z. Phys. Chem., Neue Folge Board* **1977**, *101*, 14−22.
(23) Kleinman, M. H.; Bohne, C. In *Organic Photochemistry: Molecular and Supramolecular Photochemistry*; Ramamurthy, V., Schanze, K. S., Ed.; Marcel Dekker: New York, 1997; Vol. 1, pp 391−466.
(24) Van den Bergh, B.; Boens, N.; De Schryver, F. C.; Ameloot, M.; Kowalczyk, A. *Chem. Phys.* **1992**, *166*, 249−258.
(25) Jackson, G.; Porter, G. *Proc. R. Soc. London A.* **1961**, *260*, 13−30.
(26) Lehn, J.-M. *Angew. Chem., Int. Ed. Engl.* **1988**, *27*, 89−112.
(27) McGarry, P. F.; Cheh, J.; Ruiz-Silva, B.; Hu, S.; Wang, J.; Nakanishi, K.; Turro, N. J. *J. Phys. Chem.* **1996**, *100*, 646−654.
(28) Ottaviani, M. F.; Montalti, F.; Romanelli, M.; Turro, N. J.; Tomalia, D. A. *J. Phys. Chem.* **1996**, *100*, 11033−11042.
(29) Lachish, U.; Ottolenghi, M.; Stein, G. *Chem. Phys. Lett.* **1977**, *48*, 402−406.
(30) Ju, C.; Bohne, C. *J. Phys. Chem.* **1996**, *100*, 3847−54.
(31) Barros, T. C.; Stefaniak, K.; Holzwarth, J. F.; Bohne, C. *J. Phys. Chem. A* **1998**, *102*, 5639−5651.
(32) Liao, Y.; Bohne, C. *J. Phys. Chem.* **1996**, *100*, 734−743.
(33) Scaiano, J. C.; Selwyn, J. C. *Can. J. Chem.* **1981**, *59*, 2368−2372.
(34) Mohtat, N.; Cozens, F. L.; Scaiano, J. C. *J. Phys. Chem. B* **1998**, *102*, 7557−7562.
(35) Turro, N. J.; Okubo, T.; Chung, C.-J. *J. Am. Chem. Soc.* **1982**, *104*, 1789−1794.
(36) Almgren, M.; Grieser, F.; Thomas, J. K. *J. Am. Chem. Soc.* **1979**, *101*, 279−291.
(37) Zhao, Z.; Sun, L.; Crooks, R. M. *J. Am. Chem. Soc.* **1998**, *120*, 4877−4878.
(38) Balogh, L.; Tomalia, D. A. *J. Am. Chem. Soc.* **1998**, *120*, 7355−7356.
(39) Ottaviani, M. F.; Montalti, F.; Turro, N. J.; Tomalia, D. A. *J. Phys. Chem. B* **1997**, *101*, 158−166.
(40) Windholz, M.; Budavari, S.; Blumetti, R. F.; Otterbein, E. S. *The Merck Index*, 10th ed.; Merck & Co., Inc.: Rahway, NJ, 1983.
(41) Taft, R. W.; Wolf, J. F.; Beauchamp, J. L.; Scorrano, G.; Arnett, E. M. *J. Am. Chem. Soc.* **1978**, *100*, 1240−1249.
(42) Tedesco, A. C.; Nogueira, L. C.; Carreiro, J. C.; da Costa, A. B.; Bonilha, J. B. S.; Moreira, P. F.; Alonso, E. O.; Quina, F. H. *Langmuir* 2000, *16*, 134−140.